ELSEVIER

Journal of Nuclear Materials 258–263 (1998) 985–989

journal of nuclear materials

Calculation and measurement of helium generation and solid transmutants in Cu–Zn–Ni alloys

L.R. Greenwood [a,*], B.M. Oliver [a], F.A. Garner [a], T. Muroga [b]

[a] *Pacific Northwest National Laboratory* [1], *P.O. Box 999, Richland, WA 99352, USA*
[b] *National Institute for Fusion Science, Toki, Gifu 509-52, Japan*

Abstract

A method recently proposed by Garner and Greenwood [1] would allow the separation of the simultaneous and possibly synergistic effects of solid and gaseous transmutation in Cu–Zn–Ni alloys. Copper transmutes primarily to Ni and Zn, leading to an accelerated production of helium from the ingrowth of zinc in mixed-spectrum reactors. Adding Zn to Cu alloys eliminates the time required for this ingrowth and leads to accelerated helium rates which are comparable to the well-known effect in Ni. Using a suitable Cu–Zn–Ni alloy matrix in a comparative irradiation of thermal neutron shielded and unshielded specimens, the separate influences of the solid and gaseous transmutants should be distinguishable. To assess the potential of this proposal, it is necessary to show that we can accurately predict the isotopic and elemental evolution of these alloys. In the current study, several different Cu–Zn–Ni alloys, irradiated in the HFIR JP-23 experiment, were characterized by measuring of the helium content as well as the solid transmutants. The measured values are in good agreement with calculations based on neutron dosimetry, therefore allowing the successful design of the transmutation experiment proposed by Garner and Greenwood. © 1998 Published by Elsevier Science B.V. All rights reserved.

1. Introduction and background

The production of helium and solid transmutation products in irradiated materials can have a significant impact on the material's properties. Fusion reactors produce more helium and somewhat different levels of solid transmutants in most elements than do fission reactors because of the significant flux of 14 MeV fusion neutrons [2]. Ni has accelerated helium production in fission reactors because of a thermal neutron (n,α) reaction of ^{59}Ni produced by the ^{58}Ni(n,γ) reaction [3]. Copper is also known to have accelerated helium production in fission reactor irradiations; however, the production rates are much lower than for Ni since a three-step reaction is required, i.e., ^{63}Cu(n,γ)^{64}Cu(β)^{64}Zn(n,γ)^{65}Zn(n,α) [4]. Adding natural Zn directly to Cu alloys eliminates the need for ingrowth from Cu, and, therefore, helium production is accelerated from ^{64}Zn, which has a 48.6% abundance. However, the net helium production rate from Zn is about 5% that from Ni, since the cross sections and isotopic abundances (^{64}Zn vs. ^{58}Ni) are lower. Nickel is also produced by transmutation from Cu, and both Ni and Zn can affect the various physical properties of interest as well as contribute to gas production. Garner and Greenwood [1] have proposed that a matrix of Cu–Ni–Zn alloys could be used to study the separate and possibly synergistic influences of both helium and solid transmutants. This method envisions using and comparing results from both thermal-neutron shielded and unshielded irradiations.

To test this idea, various Cu–Zn–Ni alloys, including Cu–5Ni, Cu–3.5Zn, and Cu–2Mn were fabricated in Japan and irradiated in the High Flux Isotopes Reactor (HFIR). Measurements of the helium production in these alloys were then compared with dosimetry-based calculations. Solid transmutation of the alloy starting

* Corresponding author. Tel.: +1-509 376 6918; fax: +1-509 372 2156; e-mail: lr_greenwood@pnl.gov.

[1] Pacific Northwest National Laboratory is operated by the US Department of Energy by Battelle under Contract DE-AC06-76RLO 1830

0022-3115/98/$19.00 © 1998 Published by Elsevier Science B.V. All rights reserved.
PII: S0022-3115(98)00085-3

materials produced significant levels of Co, Fe, Mn, Cr, and V. These transmutants were measured by a variety of techniques for comparison to theoretical calculations.

2. Neutron dosimetry for HFIR JP-23 irradiation

The alloys were irradiated in the JP-23 experiment in the G6 target position of the HFIR from 16 December, 1993, to 3 June, 1994, for a net exposure of 110.2 effective full power days at 85 MW. The design and material loading, including the locations of the various Cu alloys, is documented in a report by Ermi and Gelles [5]. Neutron dosimetry packages were included in the experiment, and the measured results and radiation damage calculations were reported by Greenwood and Ratner [6]. These measured neutron fluences and energy spectra were used as the basis for the transmutation calculations. The midplane total neutron fluence was 4.39×10^{22} n/cm^2 with a thermal component of 1.92×10^{22} n/cm^2 (<0.5 eV). The alloys were irradiated at two different temperatures, 400°C (8.8–12.0 cm above the core midplane) and 300°C (13.0–16.2 cm above midplane). The elevations of the samples are provided in Tables 2–4. Neutron fluence gradients are described by the equation $f(x) = f(0)\ (1 - 1.139 \times 10^{-3}\ x^2)$, where x is the vertical distance from reactor centerline in cm.

3. Characterization of starting materials

To determine the transmutation effects, these alloys were characterized both before and after irradiation. The compositions of the unirradiated alloys, as measured by X-ray fluorescence (XRF), are listed in Table 1. The concentrations of the principal constituents are close to the nominal values; however, the sometimes-small differences can be quite important for proper interpretation of the subsequent transmutation calculations. Uncertainties in the measurements are typically on the order of ±5%, except for a 25% uncertainty for Fe in the Cu–2Mn alloy. Calculations do not agree very well with the Mn contents of the Cu–2Mn alloy, as will be discussed later.

4. Helium measurements and calculations

Duplicate milligram-sized sections of eight of the irradiated alloy samples were analyzed for helium content using isotope-dilution mass spectrometry, following vaporization in a resistance-heated graphite crucible in a high-temperature vacuum furnace. Details of the technique have been published previously [7]. The absolute amount of ^{4}He released was measured relative to a known quantity of added ^{3}He "spike". The results are listed in Table 2. The predicted helium content of each alloy was calculated using the neutron dosimetry results and nuclear cross sections from Ref. [3], as shown at midplane in Fig. 1. The ^{63}Cu(n,γ) and ^{64}Zn(n,γ) thermal neutron cross sections are 4.5 b (barns) and 0.76 b, respectively. The isotope ^{64}Cu($T_{1/2} = 12.7$ h) decays 61% by electron capture to ^{64}Ni and 39% by β^- decay to ^{64}Zn. However, the thermal neutron cross sections required to calculate helium from either Cu or Zn have not been measured. Using values inferred from irradiations of Cu in various reactors [2], the thermal cross sections for the ^{64}Cu(n,γ), ^{65}Zn(n,α), and ^{65}Zn(n,absorption) reactions have been deduced to be 270 ± 170 b, 4.7 ± 0.5 b, and 66 ± 8 b, respectively. The helium production cross sections for fast neutron reactions were taken from files of evaluated data [8]. The ratios of the calculated to measured (C/M) helium values, as listed in the last column of Table 2, show very good agreement, with an average ratio of 1.04 ± 0.05. This agreement confirms the validity of the deduced thermal cross sections, as given above.

5. Radioactivity measurements

The irradiated alloys were analyzed for radionuclide content, using both direct gamma spectrometry and nuclear counting after wet chemical separations. The activities listed in Table 3 are generally accurate to ±5%, except for ^{54}Mn in the Cu–2Mn alloy where the uncertainty is ±15%. The activities of various radionuclides can be compared directly to calculations based on the initial compositions in Table 1 and the neutron dosimetry, as will be discussed later. Both ^{59}Ni and ^{65}Zn are very important for helium production since they both

Table 1
XRF analyses of copper alloys (wt%)

Element	Cu	Cu–5Ni	Cu–3.5Zn	Cu–5Ni–2Zn	Cu–2Mn
Cue	100.0	94.1	95.9	91.0	98.1
Ni	<0.030	5.49	<0.027	5.74	<0.027
Zn	<0.070	<0.076	3.80	2.60	<0.061
Mn	<0.013	<0.012	<0.012	<0.010	1.63
Fe	<0.012	<0.012	<0.011	<0.010	0.041

Table 2
Helium measurements and calculations

Material	Height (cm)	Mass [a] (mg)	Measured ^{4}He 10^{13} atoms	Helium concentration (appm) [b]			Ratio *C*/*E*
				Measured	Average [c]	Calculated [d]	
Cu	13.4	1.196	4.357	3.844	3.84	4.23	1.10
		1.087	3.957	3.841	±0.01		
Cu–3.5Zn	13.8	2.560	18.90	7.798	8.16	8.07	0.99
		2.813	23.72	8.907	±0.65		
		1.156	8.507	7.773			
Cu–5Ni–2Zn	10.1	2.631	454.6	181.7	182	181	1.00
		1.010	175.3	182.5	±1		
Cu–5Ni–2Zn	13.9	2.179	304.1	145.4	146	160	1.09
		2.138	299.7	147.4	±1		
Cu–3.5Zn	9.8	2.847	24.35	9.034	8.83	9.18	1.04
		0.864	6.621	8.095	±0.66		
		1.715	15.19	9.356			
Cu [e]	9.1	2.048	9.016	4.645	4.64	4.82	1.04
		2.176	9.572	4.642	±0.01		
Cu–5Ni [e]	9.5	1.155	195.4	177.8	179	173	0.97
		0.365	62.44	179.8	±1		
Cu–5Ni [e]	13.6	0.904	122.8	142.8	141	152	1.08
		0.447	58.77	138.2	±3		

[a] Mass of specimen for analysis. Mass uncertainty is ±0.002 mg.
[b] He concentration in appm (10^{-6} atom fraction) with respect to the total atoms in the specimen.
[c] Mean and standard deviation (1σ) of replicate analyses.
[d] Calculations are based on neutron dosimetry in Ref. [6].
[e] Thinned central region.

are known to have thermal (n,α) cross sections large enough to greatly accelerate helium production in mixed spectrum reactors. Some of the radionuclides are only produced by one of the starting elements in the alloy, such as ^{57}Co and ^{59}Ni from Ni and ^{54}Mn from Mn. The analysis of other reaction products is more complicated, however, since multiple nuclear reactions are involved. For example, ^{63}Ni is produced by the ^{63}Cu(n,p) and ^{62}Ni(n,γ) reactions, ^{60}Co is produced by the ^{63}Cu(n,α), ^{60}Ni(n,p), and ^{58}Ni(n,p)^{58}Co(n,γ)^{59}Co(n,γ) reactions, and ^{65}Zn is produced by the ^{64}Zn(n,γ) and ^{63}Cu(n,γ)^{64}Cu(β)^{64}Zn(n,γ) reactions.

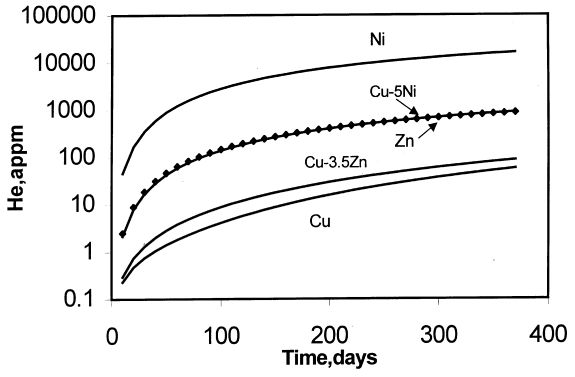

Fig. 1. Production of helium vs. time in HFIR for pure elements and alloys.

6. Elemental concentrations in irradiated alloys

The elemental concentrations of the irradiated alloys were determined using a combination of the activation data in Table 2 and elemental analysis by inductively coupled plasma mass spectrometry (ICP-MS). Small pieces of each alloy were dissolved in acid and vaporized in the ICP-MS analyses. The results of these analyses are listed in Table 4. Uncertainties are typically ±10%.

7. Comparison of measured and calculated solid transmutation

The measured radioactivities and weight fractions listed in Tables 3 and 4 can be compared with calculations based on neutron dosimetry, evaluated nuclear cross sections, and the starting compositions of the alloys, as listed in Table 1. Such calculations are complicated because of competing reactions, as discussed earlier. In addition, nuclear burnup effects can be quite substantial because of the high thermal neutron flux in HFIR. In several cases, the nuclear cross sections required for such calculations are not well known or have a large uncertainty. The principal solid transmutants from Cu are Zn and Ni. The ICP-MS measurements in Table 4 include calculations of the ^{64}Zn and ^{64}Ni production levels since it was not possible to separate these

Table 3
Measured activities in copper alloys (μCi/mg at 6/3/94)

Alloy	Height (cm)	^{59}Ni	^{63}Ni	^{60}Co	^{65}Zn	^{57}Co	^{54}Mn
Cu	13.1	$<4 \times 10^{-4}$	4.00×10	2.07×10	4.77×10^{2}	$<1 \times 10^{-1}$	$<4 \times 10^{-1}$
Cu	9.0	$<5 \times 10^{-4}$	4.35×10	2.29×10	5.97×10^{2}	$<2 \times 10^{-1}$	$<4 \times 10^{-1}$
Cu–5Ni	13.7	7.51×10^{-2}	1.91×10^{1}	6.82×10	4.36×10^{2}	1.83×10^{-1}	$<4 \times 10^{-2}$
Cu–5Ni	9.6	7.57×10^{-2}	2.02×10^{1}	8.52×10	5.49×10^{2}	1.83×10^{-1}	$<5 \times 10^{-2}$
Cu–3.5Zn	13.9	$<3 \times 10^{-4}$	3.68×10	1.94×10	1.21×10^{3}	$<2 \times 10^{-1}$	$<6 \times 10^{-1}$
Cu–3.5Zn	9.9	$<4 \times 10^{-4}$	3.97×10	2.21×10	1.41×10^{3}	$<2 \times 10^{-1}$	$<5 \times 10^{-1}$
Cu–2Mn	14.7	$<3 \times 10^{-4}$	3.82×10	2.03×10	4.29×10^{2}	$<6 \times 10^{-2}$	1.58×10^{-1}
Cu–2Mn	11.0	$<3 \times 10^{-4}$	3.95×10	2.17×10	5.31×10^{2}	$<7 \times 10^{-2}$	1.46×10^{-1}

Table 4
Measured composition of irradiated alloys (wt%)

Alloy	Height (cm)	Zn	Ni	Co	Fe	Mn	Cr	V
Cu	13.1	3.1	2.8	<0.02	<0.01	0.08	0.33	0.1
Cu	9.0	3.4	3.2	0.11	<0.01	0.08	0.33	0.1
Cu–5Ni	13.7	3.0	7.2	0.12	<0.01	0.05	0.07	<0.02
Cu–5Ni	9.6	3.7	8.1	<0.02	<0.01	0.06	0.07	0.02
Cu–3.5Zn	13.9	6.3	2.7	<0.02	<0.01	0.06	0.07	<0.02
Cu–3.5Zn	9.9	4.4	3.0	<0.02	<0.01	0.06	0.05	<0.02
Cu–2Mn	14.7	4.7	2.7	<0.02	0.30	1.53	0.05	<0.02
Cu–2Mn	11.0	4.1	3.2	<0.02	0.34	1.57	0.07	<0.02

two isotopes using this technique. A discussion of these reactions was published previously in Ref. [15]. A comparison of measurements and calculations for other reaction products is shown in Table 5.

As can be seen from Table 5, the measured production of various radioactive isotopes is in good agreement with the calculations. The *C*/*M* ratios show a tendency for overprediction, which may be caused by neutron self-shielding effects that are not properly accounted for in these calculations because an accurate model of the geometric irradiation conditions is lacking. However, the *C*/*M* ratios generally fall well within the combined uncertainties of both the measurements and calculations.

The calculated burnup of Mn to Fe via the ^{55}Mn(n,γ)^{56}Mn(β^{-})^{56}Fe reaction differs significantly from the measured burnup. This reaction has a 13.3 b thermal neutron cross section leading to significant burnup in the high HFIR thermal neutron flux. The calculations predict that the Mn should be depleted by

Table 5
Comparison of measured and calculated solid transmutation

Starting element	Reaction/product	Units	Measured	Calculated	Ratio *C*/*M*
Ni	^{58}Ni(n,γ)^{59}Ni	μCi/mg	7.51×10^{-2}	9.11×10^{-2}	1.21
			7.57×10^{-2}	9.63×10^{-2}	1.27
Ni	^{62}Ni(n,γ)^{63}Ni [a]	μCi/mg	1.53×10^{1}	1.71×10^{1}	1.12
			1.61×10^{1}	1.87×10^{1}	1.16
Cu	^{63}Cu(n,γ)^{64}Zn	μCi/mg	1.21×10^{3}	1.35×10^{3}	1.12
	^{64}Zn(n,γ)^{65}Zn		1.41×10^{3}	1.54×10^{3}	1.09
Cu	^{63}Cu(n,α)^{60}Co	μCi/mg	2.07×10	2.54×10	1.16
			2.29×10	2.86×10	1.17
Mn [b]	^{55}Mn(n,2n)^{54}Mn	μCi/mg	1.58×10^{-1}	1.43×10^{-1}	0.91
			1.46×10^{-1}	1.61×10^{-1}	1.10
Mn [c]	Burnup	Fractional burnup	0.94	0.83	0.89
			0.96	0.85	0.88
	Mn to Fe	wt%	0.26	0.24	0.92
			0.30	0.27	0.90

[a] The contribution from ^{63}Cu(n,p)^{63}Ni was subtracted using the pure Cu results.
[b] The 54Mn activity measurements have an uncertainty of ±15%.
[c] See text concerning interpretation of Mn and Fe data.

15–17%. However, the initial XRF data compared to the irradiated ICP-MS data show burnups of only 4–6%. Comparison of the Fe content of the Cu–2Mn alloy between the initial and irradiated conditions shows an increase from 0.041 wt% to 0.30–0.34 wt%, in reasonable agreement with the calculations of the burnup of Mn to Fe, especially considering the large uncertainty of ±25% in the XRF measurement of Fe in the starting material. The agreement between measurements and calculations for the ingrowth of Fe suggests that there may be a problem with the Mn measurements. Assuming that the XRF Mn measurement in the unirradiated Cu–2Mn alloy is correct, then the ICP-MS measurements of Mn in the irradiated alloy may be biased high, possibly because of interference effects.

All of the other solid transmutants listed in Table 4, namely Co, Cr, and V, cannot be explained by known transmutation reactions. All of these values are close to the ICP-MS detection limits, and the data may thus be explained either as an artifact of the technique or as arising from very low impurities in some of the starting materials.

8. Conclusions and future work

Detailed calculations for the main solid and radioactive transmutation products are complicated because of multiple contributions from competing reactions from the principal elements, as discussed above. However, the calculations appear to be in good agreement with the measurements. This agreement of measured and calculated helium production and solid transmutation demonstrates that we understand the nuclear reaction mechanisms and dosimetry-based neutron metrology. The nuclear data are also validated. The significant levels of transmutation in Cu alloys and other materials have important consequences for material property evolution under irradiation, as are discussed in Ref. [1] and other papers at this conference [9–12]. Transmutation effects must be taken into account for many different fusion reactor materials, both for the study of property changes in fission reactor irradiations and the prediction of such effects for future fusion reactors. Some of the Cu alloys examined in this paper, along with other alloys, have also been studied in fast reactors where the transmutation rates are significantly different; however, transmutation has still been invoked to explain the observed irradiation response of the alloys [1,13–18].

The helium and solid transmutation products have been shown to vary considerably in concentration according to the composition of the Cu-based alloys used in this study. It does appear, however, relatively straightforward to measure and predict the levels of transmutants to be produced in any given neutron spectra. Using a suitable matrix of Cu–Zn–Ni alloys, it therefore appears that a comparative irradiation involving both thermal neutron-shielded and unshielded specimens can be designed to distinguish the separate and possibly synergistic influences of solid and gaseous transmutants on various material properties of Cu alloys.

References

[1] F.A. Garner, L.R. Greenwood, Proceedings of Ishino Conference on Fundamentals of Radiation Damage and Challenges for Future Nuclear Materials, 1995, Tokyo, Japan (in press).
[2] F.A. Garner, H.L. Heinisch, R.L. Simons, F.M. Mann, Radiat. Def. Solids 113 (1990) 224.
[3] L.R. Greenwood, J. Nucl. Mater. 116 (1983) 137.
[4] D.W. Kneff, L.R. Greenwood, B.M. Oliver, R.P. Skowronski, E.L. Callis, Radiat. Eff. 92–96 (1985) 553.
[5] A.M. Ermi, D.S. Gelles, Fusion Reactor Materials Semiannual Progress Report, DOE-ER-0313/17 (1995) 35–49.
[6] L.R. Greenwood, R.T. Ratner, Fusion Reactor Materials Semiannual Progress Report, DOE-ER-0313/21 (1997) 229–232.
[7] H. Farrar, B.M. Oliver, J. Vac. Sci. Technol. A 4 (1986) 1740.
[8] Gas Production File 533, Evaluated Nuclear Data File, Version V, Part B, National Nuclear Data Center, Brookhaven National Laboratory.
[9] F.A. Garner, B.M. Oliver, L.R. Greenwood, these Proceedings.
[10] T. Muroga, H. Watanabe, N. Yoshida, these Proceedings.
[11] S. Ohnuki, F.A. Garner, L.R. Greenwood, N. Sekimura, Y. Kohno, T. Muroga, A. Hasegawa, H. Takahashi, K. Abe, presented at 8th Int. Conf. on Fusion Reactor Materials, Sendai, Japan, 1997.
[12] T. Muroga, N. Yoshida, J. Nucl. Mater. 212–215 (1994) 266.
[13] T. Muroga, F.A. Garner, J. Nucl. Mater. 207 (1993) 327.
[14] H. Watanabe, F.A. Garner, J. Nucl. Mater. 212–215 (1994) 370.
[15] D.J. Edwards, F.A. Garner, L.R. Greenwood, J. Nucl. Mater. 212–215 (1994) 404.
[16] F.A. Garner, M.L. Hamilton, T. Shikama, D.J. Edwards, J.W. Newkirk, J. Nucl. Mater. 191–194 (1992) 386.
[17] D.J. Edwards, K.R. Anderson, F.A. Garner, M.L. Hamilton, J.F. Stubbins, A.S. Kumar, J. Nucl. Mater. 179–181 (1991) 250.
[18] F.A. Garner, H.R. Brager, K.R. Anderson, J. Nucl. Mater. 179–181 (1991) 250.